Pharmacophore modeling and parallel screening for PPAR ligands

Patrick Markt · Daniela Schuster · Johannes Kirchmair ·
Christian Laggner · Thierry Langer

Abstract   We describe the generation and validation of pharmacophore models for PPARs, as well as a large scale validation of the parallel screening approach by screening PPAR ligands against a large database of structure-based models. A large test set of 357 PPAR ligands was screened against 48 PPAR models to determine the best models for agonists of PPAR-α, PPAR-δ, and PPAR-γ. Afterwards, a parallel screen was performed using the 357 PPAR ligands and 47 structure-based models for PPARs, which were integrated into a 1537 models comprising in-house pharmacophore database, to assess the enrichment of PPAR ligands within the PPAR hypotheses. For these purposes, we categorized the 1537 database models into 181 protein targets and developed a score that ranks the retrieved targets for each ligand. Thus, we tried to find out if the concept of parallel screening is able to predict the correct pharmacological target for a set of compounds. The PPAR target was ranked first more often than any other target. This confirms the ability of parallel screening to forecast the pharmacological active target for a set of compounds.

P. Markt · D. Schuster · J. Kirchmair · C. Laggner · T. Langer
(✉)
Department of Pharmaceutical Chemistry, Institute of Pharmacy and Center for Molecular Biosciences Innsbruck (CMBI), University of Innsbruck, Innrain 52c, 6020 Innsbruck, Austria
e-mail: Thierry.Langer@uibk.ac.at

D. Schuster · J. Kirchmair · T. Langer
Inte:Ligand Softwareentwicklungs- und Consulting GmbH, Clemens Maria Hofbauer-Gasse 6, 2344 Maria Enzersdorf, Austria

Introduction

Peroxisome proliferator-activated receptors (PPARs) are fatty acid activated transcription factors that belong to the steroid/retinoid nuclear receptor family. The three PPAR subtypes PPAR-α (NR1C1), PPAR-δ (NR1C2), and PPAR-γ (NR1C3) found in mammals play a decisive role in glucose and lipid homeostasis.

PPAR-α is a regulator of fatty acid metabolism and energy homeostasis [1]. Mainly expressed in the liver and adipose tissue, PPAR-α activates the lipoprotein lipase (LPL) by upregulation of gene transcription and by downregulation of apolipoprotein C-III, which is an inhibitor of LPL and therefore decreases serum triglyceride levels. In addition, circulating HDL is increased by PPAR-α agonists. Moreover, PPAR-α activation improves glucose tolerance and causes regression of atherosclerotic lesions by decreasing cytokines and proteins that are necessary for monocyte activation and fatty acid metabolism [2]. Finally, agonists of PPAR-α reduce weight gain by either improvement of fatty acid metabolism or by increasing energy expenditure which makes PPAR-α an anti-obesity target for research and development [3]. The fibrates be-clofibrate, bezafibrate, ciprofibrate, clofibrate, fenofibrate, and gemfibrozil are FDA-approved PPAR-α agonists that are currently used in the treatment of dyslipidemia.

PPAR-γ is expressed in adipose tissue. Agonists of this subtype increase adipocyte differentiation and improve the storage of fatty acids. Furthermore, they enhance insulin

sensitivity by a not fully understood mechanism that involves PPAR-γ activity in adipose tissue, in skeletal muscle, and in the liver. Some thiazolidinediones (TZDs), such as the FDA-approved drugs rosiglitazone (Avandia) and pioglitazone (Actos), are PPAR-γ agonists that are used for the treatment of type 2 diabetes [2]. However, TZDs increase body weight by causing triglyceride accumulation during adipogenesis [4]. To reduce this side effect, partial agonists of PPAR-γ with anti-diabetic effects are developed. Finally, TZDs and other PPAR-γ agonists are known to have anti-atherogenic effects [2].

The ubiquitously expressed PPAR-δ acts as a central regulator of fat burning and activator of thermogenesis. Activation of PPAR-δ increases fatty acid oxidation and energy expenditure, improves glucose tolerance, and inhibits inflammatory processes. Therefore, PPAR-δ agonists could be used for the therapy of diet-induced obesity and type 2 diabetes. Their therapeutic use as anti-atherogenic drugs is undetermined [2].

Structure of PPARs

The functional domains of PPARs are N-terminal, DNA-binding (DBD) and ligand-binding (LBD). The DNA-binding domain of the three PPAR subtypes is highly conserved, whereas the ligand-binding domains differ significantly [5]. To regulate the expression of genes, they interact with DNA-responsive elements that include hexanucleotide sequence AGGTCA repeats within promotor regions of the target genes after heterodimerization with 9-cis retinoic acid receptors (RXRs) [5, 6]. When no ligand is present, corepressor complexes (nuclear receptor corepressor and silencing mediator for retinoid and thyroid receptors) are recruited which inhibit transcription. Agonists that bind to PPARs lead to recruitment of coactivator proteins that activate transcription. In addition, PPARs block activities of signal-dependent transcription factors, such as NF-κB and activator protein 1 which also represses gene transcription [2].

Ligand–protein interactions

The endogenous agonists of PPARs are fatty acids. Accordingly, the binding site is mostly hydrophobic. Also synthetic PPAR ligands establish several hydrophobic interactions with the three arms of the Y-shaped ligand-binding domain [1, 7]. The LBDs of the three PPAR subtypes are very large and bind a multitude of natural and synthetic ligands. PPAR-α has the largest and most hydrophobic pocket, followed by PPAR-γ and PPAR-δ. Moreover, the PPAR-α ligand-binding domain seems to be predestined for

binding hydrophobic fatty acids, whereas the more polar PPAR-γ pocket favors hydroxylated fatty acid ligands. The pocket of PPAR-δ differs substantially from the LBDs of PPAR-α and PPAR-γ, especially in the area next to the activation function helix 2 (AF-2 helix, also called α12). It cannot accommodate large hydrophobic groups linked to the agonist's hydrophilic head group because of its small size. Thus, agonists for PPAR-δ that lack these large appendages are far more subtype-selective than agonists of the other two PPAR isoforms. Generally, the PPAR binding sites consist of three arms: Arm I exhibits mainly polar character and includes the AF-2 helix that contains the transcriptional activation domain. The hydrophilic head group of the PPAR agonist interacts with this part of the pocket, whereas the hydrophobic tail of the PPAR ligand is either buried in the hydrophobic arm II (tail up pocket) or in arm III that is formed by hydrophobic and hydrophilic residues (entrance region of the pocket, tail down pocket, see Table 1).

Some agonists such as GW409544 are able to bind to both hydrophobic arms because of their branched structure. In contrast to the shape of arm II, the structure of arm III is conserved among the three receptor isoforms. Accordingly, subtype selectivity depends on the topology of arm I and II [1, 7, 8].

Generally, *PPAR ligands* contain a hydrophilic group (carboxylic acid, TZD ring, or other groups) that is essential for biological activity. It is orientated toward the AF-2 helix in the Y-shaped ligand binding pocket and forms a network of hydrogen bonds with the receptor. This network stabilizes a conformation of the AF2-helix which is important for the formation of a charge clamp. Thus, PPARs can interact with coactivator proteins that activate gene transcription. In the PPAR-γ protein, hydrogen bonds are formed between the amino acids Tyr473 and His449 and the polar head group of the agonist. Sometimes other hydrophilic interactions are established with the residues His323 and Ser289 [9]. The same amino acid residues are involved in the hydrogen bonding network in the PPAR-δ subtype [1]. In contrast, PPAR-α agonists stabilize the AF2-helix by forming hydrogen bonds with the residues Tyr464, Tyr314, and Ser280 [7]. Figure 1a–c displays the LBDs of the three PPARs, derived from the three PDB entries 1k7l (PPAR-α-agonist complex), 1y0s (PPAR-δ-agonist complex), and 2f4b (PPAR-γ-agonist complex) using LigandScout [10].

Finally, *partial agonists* of PPAR-γ are unable to form hydrogen bonds to residues that direct the AF-2 helix into its active conformation. Their interactions with the ligand-binding site are rather of hydrophobic nature. Nevertheless, the receptor adopts the active conformation in the presence of a partial agonist and binds coactivator proteins. However, in contrast to full agonists, partial agonists of PPAR-γ possess another cofactor recruitment profile. Complexes of

Table 1 Binding pocket residues of the three different PPAR subtypes [8, 34]

PPAR-α			PPAR-γ			PPAR-δ		
arm I	arm II	arm III	arm I	arm II	arm III	arm I	arm II	arm III
Phe273	Ile241	Asn219	Phe282	Ile249	Pro227	Phe282	Ile249	Asn227
Cys276	Leu247	Met220	Cys285	Leu255	Leu228	Cys285	Leu255	Met228
Gln277	Glu251	Thr279	Gln286	Glu259	Arg288	Gln286	Glu259	Thr288
Ser280	Leu254	Glu282	**Ser289**	Phe264	Glu291	Thr289	Trp264	Glu291
Tyr314	Ile272	Thr283	**His323**	Ile281	Ala292	**His323**	Val281	Thr292
Ile317	Cys275	Glu286	Ile326	Gly284	Glu295	Ile326	Arg284	Glu295
Phe318	Met330	Leu321	Tyr327	Val339	Leu330	Phe327	Leu339	Leu330
Ile354	Val332	Val324	Phe363	Ile341	Leu333	Ile363	Val341	Ile333
His440	Ile339	Ala333	**His449**	Met348	Ser342	**His449**	Val348	Ala342
Val444	Phe343	Tyr334	Leu453	Phe352	Glu343	Met453	Phe352	Asn343
Leu460	Leu344		Leu469	Leu353		Leu469	Leu353	
Tyr464	Met355		**Tyr473**	Met364		**Tyr473**	Ile364	

Residues that form hydrogen bonds with the agonists head group are highlighted in bold [1, 7, 9]

Fig. 1 (a–c) The ligand binding pockets of the three PPAR subtypes. Amino acids forming the hydrogen bond network are shown as ball and stick figures

(a) PPAR-α

(b) PPAR-δ

(c) PPAR-γ
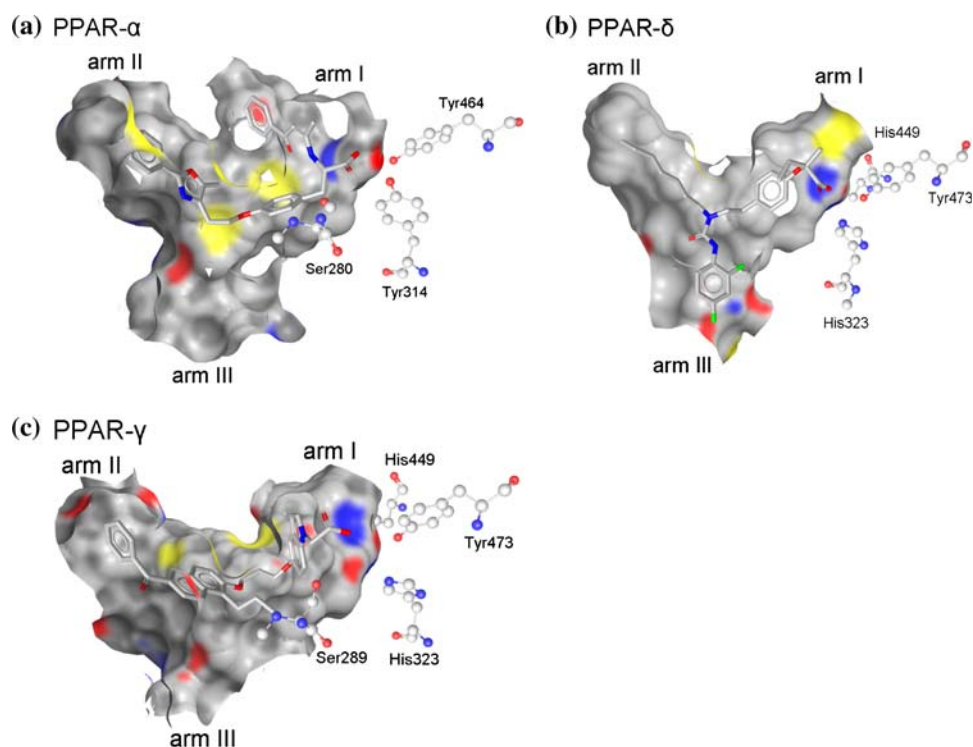
partial agonists with PPAR-γ prefer to recruit the PPAR-γ coactivator-1α (PGC1α). This coactivator leads to the expression of genes which promote insulin signaling without causing the characteristic adverse effect of triglyceride accumulation of TZDs [4, 11].

Previous approaches

Other molecular modeling studies on PPAR ligands were mainly focused on PPAR-γ agonists. 3D-QSAR studies on thiazolidine-2,4-diones and N-(2-benzoylphenyl)-l-tyrosine derivatives as PPAR-γ agonists have been performed previously with the software Apex3D to design new antidiabetic drugs. The 3D-QSAR analysis suggested that hydrogen bonds between one carbonyl oxygen atom of the ligand and PPAR-γ, as well as other hydrophilic interactions are necessary for activity [12, 13]. A docking study using the software FlexX resulted in a pharmacophore of PPAR-γ agonists that included a polar head, a hydrophobic tail, and a linker [14]. Another group used the software QUANTA/CHARMm to dock oximes into the crystal

structure of the PPAR-γ ligand-binding domain in order to identify structure-activity relationships of PPAR-γ agonists. The conclusion of this study was that potent PPAR-γ agonists adopt a tail-down configuration like rosiglitazone. Furthermore, agonists for the γ subtype possess a hydrophobic tail containing an alkyl group and an aromatic ring [15].

Aim of the study

Since not only PPAR-γ agonists, but also other PPAR ligands play an important role in many physiological processes and metabolic diseases, the aim of the first part of our study was to create pharmacophore models for PPAR-α, PPAR-γ, and PPAR-δ agonists. The resulting models were validated using a large PPAR ligand test set and a virtual database containing putative inactive ligands.

In the second part of the work we tried to validate the concept of parallel screening using the large PPAR ligand test set. Parallel screening is a newly developed in silico method to forecast the pharmacological active target for a set of compounds. For these purposes, the compounds are screened against a multitude of pharmacophore models [16]. This is automatically performed by using a Pipeline Pilot WebPort application as screening platform [17]. In order to validate the use of parallel screening for finding the correct pharmacological target for a set of compounds, we integrated all structure-based PPAR models generated in the first part of the study into our in-house database of structure-based pharmacophore models. This database— the so-called Inte:Ligand database—contains a multitude of models covering a large number of different pharmacological targets. Afterwards, we screened the large PPAR ligand test set against this pharmacophore database. Thus, we tried to investigate if the PPAR target was prioritized among the other targets of the database, in other words if the correct pharmacological target for the PPAR ligand test set was retrieved by the parallel screening approach.

Materials and methods

Hardware specifications

LigandScout 1.0 [10] and the Catalyst software package version 4.11 [18] were run on an Intel Pentium Core 2 Duo 6400 equipped with 1 GB RAM running Linux Fedora Core 6. Parallel screening using the Pipeline Pilot WebPort application was carried out on a Linux cluster equipped with Intel Pentium IV processors.

Generation of compound sets

Structures of PPAR ligands derived from literature (see Supplementary material references 1–72) were built and energetically minimized using Catalyst. The conformational models for these structures were generated within Catalyst using the following settings: Maximum number of conformers = 250, generation type = best quality, and energy range = 20 kcal/mol above the calculated lowest energy conformation. The bioactive conformations of PPAR agonists extracted from 21 Brookhaven Protein Data Bank (PDB) [19] protein–ligand complexes utilizing LigandScout were imported into Catalyst as MDL MOL-files.

Each of the 47 structure-based models was derived from one of these 21 PDB protein-PPAR agonist complexes. For the generation of the ligand-based models several compound sets were compiled utilizing PPAR agonists from the corresponding PPAR agonist training sets.

The four PPAR agonist training sets were composed of the PPAR agonists extracted from the 21 PDB complexes and PPAR agonists found in literature. The training sets were screened to refine the corresponding PPAR-α agonist, PPAR-γ agonist, PPAR-γ partial agonist, and PPAR-δ agonist pharmacophore models: (i) 18 PPAR agonists were used for the generation of the PPAR-α agonist training set, (ii) 21 PPAR agonists were forming the training set for PPAR-γ agonist models, (iii) the PPAR-γ partial agonist training set was composed of five compounds, (iv) the PPAR-δ agonist training set included seven PPAR agonists. As mentioned before, training set compounds were used to derive ligand-based models. For these models, the remaining training set compounds which did not contribute to the model generation, were utilized for model refinement. Correspondingly, for structure-based models all training set ligands except the one extracted from the PDB complex from which the model was derived, were selected to refine the model.

In addition to the four PPAR agonist training sets, also the Derwent World Drug Index 2003 (Derwent WDI), containing 63307 biologically active compounds including all marketed drugs, was utilized for 3D database screening in order to refine our pharmacophore hypotheses [20]. For each compound of the Derwent WDI the conformational model was generated within Catalyst using a maximum of 100 conformers per structure, the fast generation algorithm and an energy range of 20 kcal/mol.

All the other PPAR ligands derived from references 1–72 in the Supplementary material which were not used for the compilation of the four trainings sets were utilized for the generation of the PPAR ligand test set.

The PPAR ligand test set was used for the validation of the pharmacophore models. It includes 357 structurally

diverse PPAR ligands which were divided into 321 PPAR agonists and 36 PPAR inactives. According to literature, most of the PPAR actives are not fully selective in vitro. Therefore, the PPAR agonists of the four trainings sets and of the PPAR ligand test set were further categorized into PPAR-α agonists, PPAR-α/-γ agonists, PPAR-α/-δ agonists, PPAR-γ agonists, PPAR-γ/-δ agonists, PPAR-γ partial agonists, PPAR-δ agonists, and PPAR pan agonists. The distribution of the different PPAR agonist subtypes for each training set and for the PPAR ligand test set is shown in Table 2.

The structural diversity of the 357 test set compounds was analyzed utilizing a Pipeline Pilot script that clusters molecules based on Tanimoto similarities between a set of descriptors. Scitegic's extended connectivity fingerprints (ECFP)—a method to calculate structural fingerprints—served as descriptor set. This method indexes the environment of every atom of a compound by using up to 4 billion different structural features in order to characterize the molecule. For the analysis of the structural diversity, the setting ECFP_6 was chosen, which means that all neighbour atoms within a diameter of six bonds are considered for the feature calculation of each atom [16]. PPAR actives and PPAR inactives were investigated separately using maximum allowed dissimilarities of 0.7, 0.5, and 0.3 (Table 3).

The maximum distance of 0.7 leads to clusters of structurally diverse compounds, whereas a maximum allowed dissimilarity of 0.3 clusters more structurally related ligands. 30 clusters for PPAR actives and 9 clusters for PPAR inactives were retrieved using the least restrictive maximum allowed dissimilarity of 0.7. A larger number of clusters—174 for PPAR actives and 23 for PPAR inactives—was retrieved when the maximum distance was set to 0.3. Using this maximum distance, the largest cluster formed by PPAR actives consisted of 37

Table 3 Results of the similarity analysis for the PPAR ligand test set

Ligand set	321 PPAR agonists			36 PPAR inactives		
Maximum distance	0.7	0.5	0.3	0.7	0.5	0.3
Number of clusters	30	99	174	9	13	23

compounds. For PPAR inactives, no cluster was created which included more than eight ligands.

For further validation, a virtual database containing 12775 drug-like and diverse compounds was created with the java-based software ilib:diverse [21]. The generation of this database is described in detail in reference [22]. The conformational models for the compounds were generated utilizing the same settings for the Catalyst conformer generator catDB as mentioned above for the Derwent WDI structures (100 conformers, fast generation, energy range 20 kcal/mol). The virtual database was searched in order to determine how many "random" or putative inactive structures were able to fit into the PPAR models and to calculate enrichment factors for our hypotheses. For these purposes, the 31 PPAR-α subtype selective agonists, the 135 PPAR-γ subtype selective agonists, the five PPAR-γ partial agonists and the 17 PPAR-δ subtype selective agonists of the PPAR ligand test set were utilized as subsets of actives for the corresponding PPAR-α, PPAR-γ, and PPAR-δ agonist models and therefore included into the virtual database. According to references [23–25], the enrichment factor was calculated using the following equation:

$$EF = \frac{TP/n}{A/N}$$

where, EF—enrichment factor; TP—true positive hits (PPAR subtype selective agonists of the PPAR ligand test set that match the model); n—number of hits (PPAR

Table 2 PPAR ligands used for the four PPAR agonist training sets and for the PPAR ligand test set

Classification	Compound set				
	PPAR-α agonist trainings set	PPAR-γ agonist trainings set	PPAR-γ partial agonist trainings set	PPAR-δ agonist trainings set	PPAR ligand test set
PPAR-α agonist	7	0	0	0	31
PPAR-α/-γ agonist	4	6	0	0	88
PPAR-α/-δ agonist	1	0	0	0	20
PPAR-γ agonist	0	13	0	0	135
PPAR-γ/-δ agonist	0	0	0	0	1
PPAR-γ partial agonist	0	0	5	0	5
PPAR-δ agonist	0	0	0	3	17
PPAR pan agonist	6	2	0	4	24
Total PPAR agonists	18	21	5	7	321
PPAR inactives	0	0	0	0	36

subtype selective agonists of the PPAR ligand test set and inactive compounds from the virtual database that match the model); A—number of actives in database (all PPAR subtype selective agonists of the PPAR ligand test set); and N—number of compounds in database (all PPAR subtype selective agonists of the PPAR ligand test set and all inactive compounds from the virtual database).

Structure-based pharmacophore modeling with LigandScout and Catalyst

The LigandScout software was used for examination of 21 PPAR ligand–protein complexes from the PDB and for the generation of structure-based pharmacophore models. LigandScout derives a structure-based pharmacophore model from a single ligand–protein complex. The software extracts the crystal structure ligand and the surrounding amino acids from a PDB complex, analyzes the possible interactions of the crystal structure ligand with the ligand binding pocket of the protein, and automatically generates a pharmacophore model based on this information. LigandScout generates one chemical feature for each possible ligand–protein interaction. If there exist several ligand–protein interactions within a PDB complex that involve the same atom, a LigandScout model is derived that contains two or more features located at the respective atom. Since Catalyst is not able to handle more than one feature per atom, one of the features generated for the same atom was selected and the other features for the atom were deleted from the initial LigandScout model. Thus, for each of the features placed at this atom, one LigandScout model was exported, which differed from the other LigandScout models derived from the same PDB complex only in the respective feature. Therefore, more than one LigandScout model was derived from some PDB ligand–protein complexes. In this study, a total of 47 structure-based LigandScout models were generated using the crystal structural data of two PPAR-α-agonist, nine PPAR-γ-agonist, five PPAR-γ-partial agonist, and five PPAR-δ-agonist complexes from the PDB. Figure 2 shows the four letter PDB code of the 21 ligand–protein complexes. The number of models derived from each PDB entry is displayed as a bold number next to the four letter code. The resulting models were imported into the Catalyst software package and used as queries to search the corresponding training set (PPAR-α agonist, PPAR-γ agonist, PPAR-γ partial agonist, or PPAR-δ agonist training set) and the Derwent World Drug Index 2003 in order to refine the models (Fig. 2).

Finally, the virtual database and the PPAR ligand test set were screened using Catalyst to validate the final 47 structure-based models (Fig. 3).
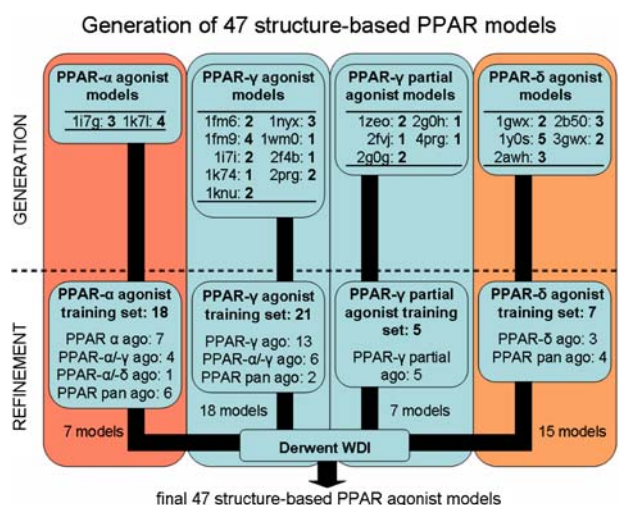
Fig. 2 PDB ligand–protein complexes used for the generation of structure-based pharmacophore models for PPAR agonists and PPAR partial agonists, as well as the corresponding PPAR agonist training sets utilized for model refinement. The bold numbers adjacent to the four letter PDB code represent the number of models generated for the ligand–protein complex

Ligand-based pharmacophore modeling with Catalyst

For PPAR-α agonists, PPAR-γ agonists, PPAR-γ partial agonists, and PPAR-δ agonists, ligand-based models were generated utilizing the HipHop algorithm of Catalyst [26]. As mentioned above, compound sets of highly active and structurally diverse PPAR agonists which were selected from the corresponding PPAR agonist training set, were used for HipHop model generation. For each of these HipHop compound sets, ten HipHop models were generated. These HipHop models were refined within Catalyst using the database search results of the corresponding PPAR agonist training set and the Derwent WDI. Since the information about the key ligand–protein interactions are
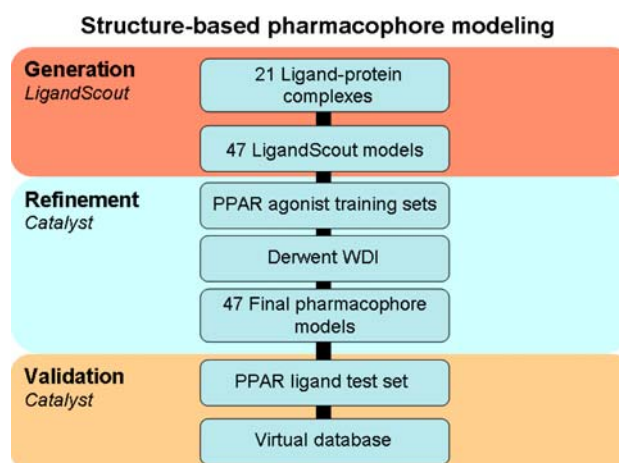

Fig. 3 Workflow for structure-based pharmacophore modeling

better described by a structure-based than a ligand-based model, we decided to select only ligand-based models which possess considerable advantages compared to the structure-based PPAR models [27]. Therefore, only one ligand-based model for PPAR-γ agonists that retrieved more hits in the PPAR-γ agonist training set than any other structure-based PPAR-γ agonist model, was used for this study. This ligand-based PPAR-γ agonist model was validated in the same way than the structure-based models by screening the PPAR ligand test set and the virtual database (Fig. 4).

Database screening with Catalyst

All 3D database searches were performed within Catalyst. This software package retrieves only structures that fit into all features of the pharmacophore model that is used as a 3D database search query. Catalyst includes two different search algorithms. The default settings of both algorithms were used. For searching the four trainings sets, the PPAR ligand test set, and the virtual database, the Best Flexible Search algorithm that generates additional conformers for the ligands during the screening process, was utilized. The Fast Flexible Search algorithm results in fewer hits by only considering the pre-computed conformers of a compound. This algorithm is normally used for searching large databases and therefore was executed for screening the Derwent WDI.

Inte:Ligand database

Our in-house pharmacophore database, the so-called Inte:Ligand database, currently consists of 1537 structure-

based models covering 181 pharmacological targets and is steadily growing. Targets comprise bacterial proteins, enzymes, receptors, signalling proteins, structuring proteins, toxins, defence proteins, and transport proteins. Among these targets, the PPAR-including nuclear hormone receptor family is represented by 18 targets: estrogen receptors (ER-α/-β), farnesoid X receptor (FXR), liver X receptors (LXR-α/-β), mineralcorticoid receptor (MR), constitutive androstane receptor (NR1l3), PPARs (PPAR-α/-δ/-γ), pregnane X receptor (PXR), retinoic acid receptors (RAR-α/-β), retinoid X receptors (RXR-α/-β), thyroid hormone receptors (TR-α/-β), and vitamin D receptor (VDR).

Parallel screening using a Pipeline Pilot WebPort application

The screening platform, which is based on a Pipeline Pilot script, uses the Fast Flexible Search algorithm of Catalyst to screen a set of ligands against a pharmacophore database. The latest version of the Inte:Ligand pharmacophore database was applied for screening, including our 47 refined and validated structure-based PPAR models. Since all of the pharmacophore models of the database were generated using structure-based pharmacophore modeling techniques, the ligand-based PPAR model was not included into the Inte:Ligand database in order to avoid biasing. Subsequently, the parallel screen was performed. The 357 PPAR ligands were screened against the Inte:Ligand database to determine their enrichment within the PPAR models of the Inte:Ligand database. Finally, the results were exported as MS Excel tables and interpreted using a perl script for workflow automation (Fig. 5).

Results

Part one: hypothesis generation and validation

A. Structure-based pharmacophore generation

Using available X-ray crystal structures from the PDB as starting points for structure-based model generation, we created pharmacophore models for PPAR-α agonists, PPAR-δ agonists, as well as PPAR-γ agonists and partial agonists. Because of a lack of published information on PPAR-α partial agonists and PPAR-δ partial agonists, no separate models for these compound classes could be generated.

In summary, 47 structure-based pharmacophore models were generated. Two models for PPAR-α agonists, one model for PPAR-γ agonists, and one model for PPAR-δ
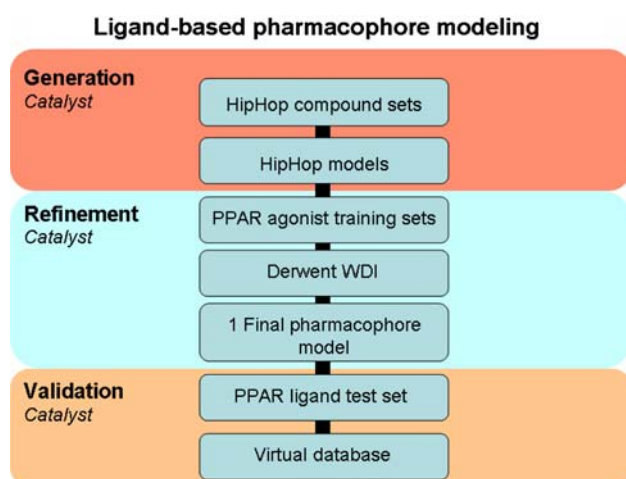

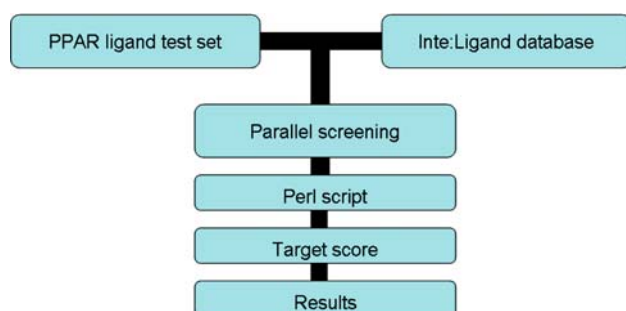**Fig. 4** Workflow for ligand-based pharmacophore modeling

Fig. 5 Parallel screening workflow

agonists represented the most selective models for PPAR agonists. These four models are discussed in the following paragraphs.

1. *PPAR-α agonists*. 1i7g and 1k7l, the two PDB entries that contain crystallographic data of PPAR-α-agonist complexes, were used for pharmacophore model generation. The most selective hypothesis was created using the PDB complex 1k7l which contains the PPAR agonist GW409544 (Table 4).

None of the 18 structures from our PPAR-α agonist training set that was used to validate and refine the hypothesis could be mapped on the initial pharmacophore model generated with LigandScout. To retrieve any of these PPAR-α test set compounds, the hypothesis was modified in Catalyst. The hydrogen bond acceptor formed between the nitrogen atom of the oxazole ring and the water molecule 194, as well as three hydrophobic features were removed. The resulting hypothesis consisted of two hydrogen bond acceptors that were situated between the carboxylic acid of the ligand and the charge clamp inducing residues Tyr314 and Tyr464, as well as three hydrophobic features located on two phenyl rings and on the methyl group of the vinylogous amide which corresponded with the bibliographic data for this PDB entry. This refined hypothesis retrieved 16 out of 18 training set compounds (89%). To reduce the number of Derwent WDI search hits, additional excluded volume spheres—areas a compound is not allowed to map—were placed at each heavy atom of the surrounding amino acids of the binding site, as detected by LigandScout. The radius of the spheres was set to 100 nm. This binding site shape was then merged with the previous model, replacing the original excluded volume spheres (Fig. 6a).

Using this so-called *PPAR-α agonist model 1* as query for a 3D database search of the Derwent WDI resulted in only 127 hits. Subsequently, the model was validated by using it as a query to search the PPAR ligand test set. Eleven out of 31 PPAR-α selective agonists (35%), seven out of 20 PPAR-α/-δ agonists (35%), 20 out of 88 PPAR-α/-γ agonists (23%), only three PPAR-γ agonists (2%), three PPAR pan agonists (13%), two PPAR inactive
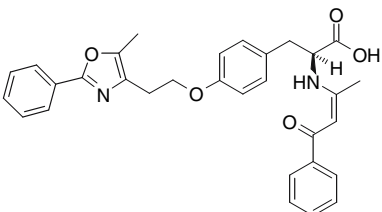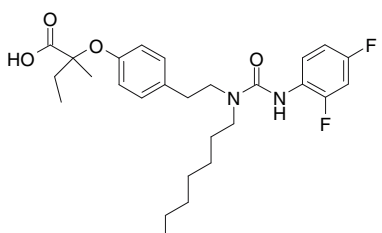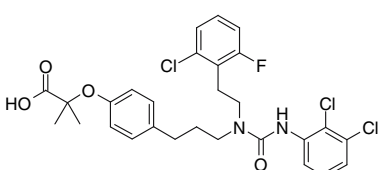
structures (6%), as well as no PPAR-γ partial agonist and no PPAR-δ agonist of the PPAR ligand test set were found. Thereafter, our virtual database, including drug-like, inactive compounds, was screened against this hypothesis. Ultimately, the enrichment of PPAR-α agonists in the 357 PPAR ligands containing test set was calculated using the number of PPAR-α selective agonists retrieved from the PPAR ligand test set and the number of inactive compounds found in the virtual database (Table 5). Because of the number of PPAR-α selective agonists, the number of PPAR-α/-δ and PPAR-α/-γ dual agonists, the small number of PPAR agonists for other subtypes retrieved from the test set, and the small number of inactives found in the virtual database, this model was chosen as our most selective model for activators of the α subtype and called *PPAR-α agonist model 1*.

PPAR-α agonist model 2—initially conceived as an agonist model for PPAR-δ—was derived from PDB entry 1y0s, a complex of the PPAR pan agonist GW2331 with PPAR-δ (Table 4). First, according to reference [1], a hydrogen bond acceptor feature located between one oxygen atom of the carboxylic acid head group and one nitrogen atom of the imidazole ring of amino acid His323 was added to the original LigandScout model. Second, to retrieve any of the seven structures from the PPAR-δ agonist training set, two hydrogen bond acceptors and six hydrophobic features were removed in Catalyst. This modified hypothesis consisted of the manually added hydrogen bond feature, a hydrogen bond acceptor formed between the other oxygen atom of the carboxylic group and residue Tyr473, as well as four hydrophobic spheres situated at the 2,4-difluorophenyl moiety, the phenoxy ring and the heptyl side chain. Lastly, to reduce the number of false positive hits, additional excluded volume spheres were created (Fig. 6b).

91 hits in the WDI and six out of seven agonists (86%) from the PPAR-δ agonist training set represent the 3D database search results of the final hypothesis. Although this model seemed to be a selective PPAR-δ agonist hypothesis, the model matched a higher percentage of PPAR-α agonists than agonists of the δ subtype when the PPAR ligand test set was searched (Table 5). 27 out of 31 PPAR-α agonists (87%), 18 out of 20 PPAR-α/-δ agonists (90%), 25 out of 88 PPAR-α/-γ agonists (28%), five out of 17 PPAR-δ agonists (29%), only eight PPAR-γ agonists (6%), 15 PPAR pan agonists (63%), one PPAR-γ partial agonist (20%), as well as five PPAR inactive structures (14%) were retrieved. Therefore, we decided to categorize this hypothesis as an unselective PPAR-α agonist model and call it *PPAR-α agonist model 2*.

Finally, we used the Catalyst software package to align *PPAR-α agonist model 1* and *PPAR-α agonist model 2* to see how similar they are. As shown in Fig. 7, the 3D

Table 4 PPAR ligands used for creation of the PPAR models

Hypothesis	PDB entry	Ref.	Ligand	Structure
PPAR-α agonist model 1	1k7l	[7]	GW409544	
PPAR-α agonist model 2	1y0s	[35]	GW2331	
PPAR-δ agonist model	1gwx	[1]	GW2433	

positions of the features of both models do not differ significantly, except for the forth hydrophobic sphere of *PPAR-α agonist model 2* that has no counterpart in the other model.

2. *PPAR-δ agonists*. Among the five PPAR-δ-agonist complexes from the PDB (1gwx, 1y0s, 2awh, 2b50, and 3gwx), the entry 1gwx contained the PPAR pan agonist GW2433 on which the best model for PPAR-δ agonists is based (Table 4). Three hydrophobic features and the hydrogen bond donor located on the urea nitrogen adjacent to the dichlorophenyl ring were deleted from the initial LigandScout model to retrieve more hits from the PPAR-δ agonist training set. The resulting model was able to match five out of seven training set compounds (71%). To further improve the selectivity, the model was merged with a shape feature created from the experimentally derived bioactive conformation of GW2433 (Fig. 6c).

The final *PPAR-δ agonist model* includes a hydrogen bond acceptor formed between the carboxylic acid group and the residue Tyr473, as well as three hydrophobic spheres situated on the three phenyl rings of the ligand. A Derwent WDI search resulted in 217 hits. Again, the model was validated by using the PPAR ligand test set and the virtual database. Nine out of 17 PPAR-δ agonists (53%), only two PPAR-α agonists (6%), one PPAR-α/-γ dual agonist (1%), one PPAR inactive structure (3%), no PPAR-γ agonist, and only 29 putative inactive compounds from the virtual database (0.23%) were found which proofed the PPAR-δ selectivity of this pharmacophore model (Table 5).

B. Ligand-based pharmacophore generation. PPAR-γ agonists

Although the PDB contains nine PPAR-γ-agonist complexes (1fm6, 1fm9, 1i7i, 1k74, 1knu, 1nyx, 1wm0, 2f4b, and 2prg) and several structure-based models were derived from these entries, the most selective PPAR-γ agonist model was the result of a ligand-based pharmacophore generation process. Different HipHop compound sets consisting of PPAR-γ agonists were utilized as input for the HipHop algorithm of Catalyst. The most promising ligand-based model was derived from a HipHop compound set of 14 structurally diverse agonists (Table 6).

Fig. 6 (**a–d**) Generation of the structure-based *PPAR-α agonist model 1* (**a**), *PPAR-α agonist model 2* (**b**), *PPAR-δ agonist model* (**c**), and the ligand-based *PPAR-γ agonist model* (**d**)
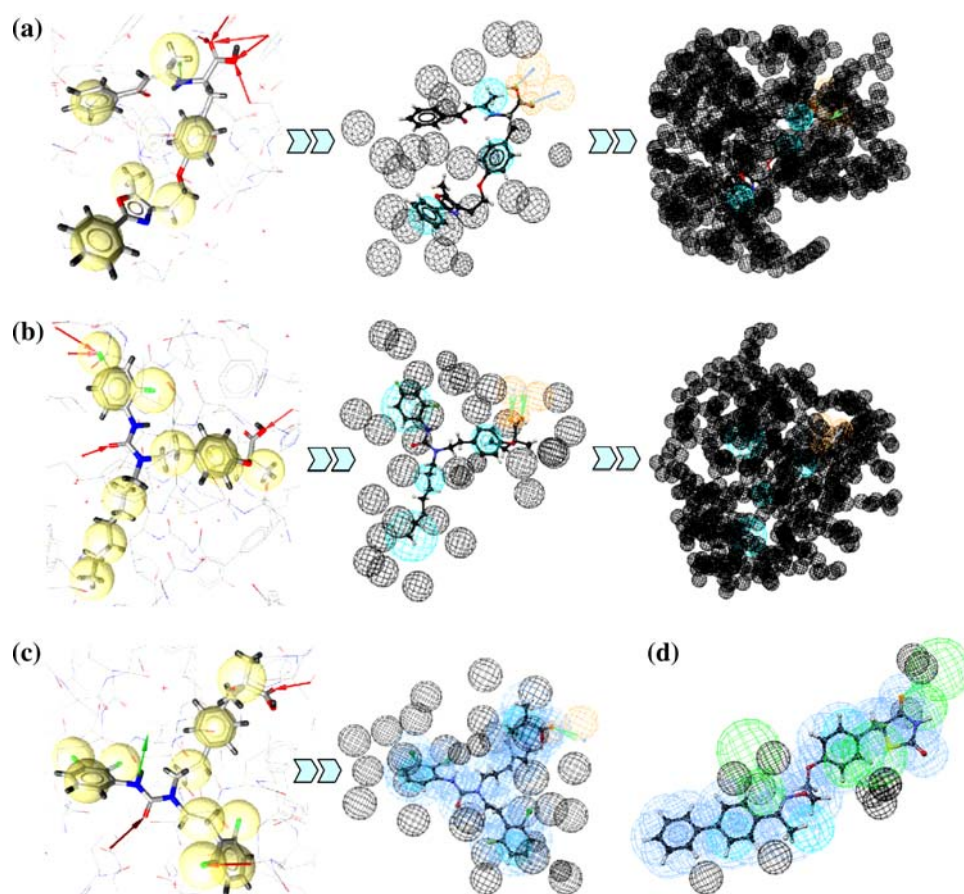
Table 5 Database search results for the PPAR models

Hypothesis	PPAR subtype selective agonists (%)	Inactives (%)[c]	Enrichment factor
PPAR-α agonist model 1	35[a]	0.06	239
PPAR-α agonist model 2	87[a]	0.23	199
PPAR-δ agonist model	53[b]	0.23	178

[a] Percentage of PPAR-α agonists found among the 31 PPAR-α agonists included in the PPAR ligands test set

[b] Percentage of PPAR-δ agonists found among the 17 PPAR-δ agonists included in the PPAR ligands test set

[c] Percentage of inactive drug-like compounds retrieved from our 12,775 compounds containing virtual database

The pharmacophore consisted of three hydrogen bond acceptors and three hydrophobic spheres. In order to reduce the number of false positive hits, a shape from compound 264908-19-2 which represented best the volume of active PPAR-γ agonists, was added to the hypothesis (Fig. 6d).

This modified model retrieved 19 of the 21 structures (91%) from the PPAR-γ agonist training set. Afterwards, the model was used as query for a Derwent WDI search which resulted in 387 hits. In order to validate the model, the PPAR ligand test set and the virtual database were searched. 44 out of 135 PPAR-γ agonists (33%), 19 out of 88 PPAR-α/-γ agonists (22%), four out of 24 PPAR pan agonists (17%), five PPAR-α agonists (16%), one PPAR-δ agonist (6%), four PPAR-α/-δ agonists (20%), ten PPAR

inactive structures (28%), and no PPAR partial agonist were retrieved from the PPAR ligand test set. Moreover, only a few putative inactive compounds from the virtual database were able to match the model (Table 7). Thus, the so-called *PPAR-γ agonist model* represented our best template for agonists of the γ subtype.

Part two: validation of the concept of parallel screening using 357 PPAR ligands

All 357 compounds from the PPAR ligand test set were screened against the whole Inte:Ligand database. This experiment should determine whether a broad screen with
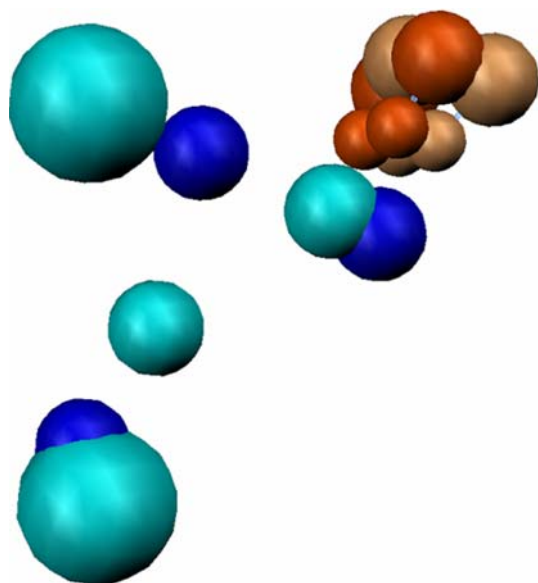
Fig. 7 Alignment of both PPAR-α agoinst models. The brown and blue spheres represent the hydrogen bond acceptors and hydrophobic features of *PPAR-α agonist model 1*, whereas the light brown and cyan spheres display the counterparts of *PPAR-α agonist model 2*

models belonging to different targets would point towards the correct pharmacological activity of a set of compounds. In other words, we tried to find out whether it is possible to prioritize the correct pharmacological target for a set of compounds if the compounds are screened against a large pharmacophore model database.

A. Definition of the target score

A perl script was used to automatically determine the number of hitting models for each target. Then we tried to find a score that ranks the targets. The problem was that some targets in the Inte:Ligand database are represented by one hundred models and more, whereas other targets are only covered by two models. This fact reflects the uneven representation of X-ray crystal structures in the PDB. While for some pharmacological targets many PDB entries exist, others are only represented by one protein–ligand complex. If we ranked the target with the highest number of hitting models first, we would discriminate against targets for which only a small number of models exist. Thus, we decided to calculate the fraction of retrieved models for each target to relate the model hits to the number of all models generated for this target [16]. However, using this score preferred targets with small model sets. For example, if a ligand was able to fit to one out of two models for target A (50%), it got a higher score than target B for which 40 out of 100 models (40%) were retrieved. Since we assume that the prediction for target B is more accurate and

therefore should be ranked higher than for target A, we weighted this score by multiplying the fraction of hitting models with the number of models found for the target to avoid a bias. In order to get easily manageable scores between 0 and 1, we formulated the following target score:

$$TS = 1 - e^{-\frac{n_{hit}^2}{n_{total}}}$$

where, TS—target score; n_{hit}—number of hitting models for a target; and n_{total}—total number of models for a target.

If none of the models for one target matched a PPAR agonist, the score for the target was 0. The theoretically highest possible score is 1 which can be only reached for an infinitely large number of models, all of which have to be hit.
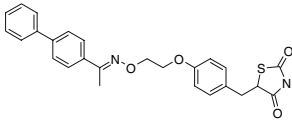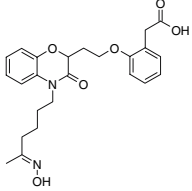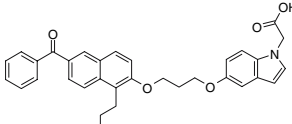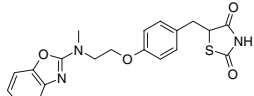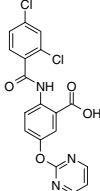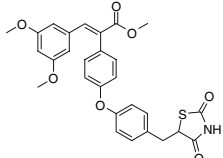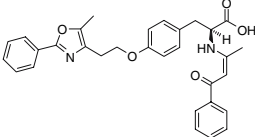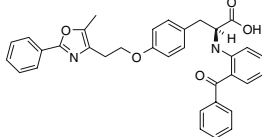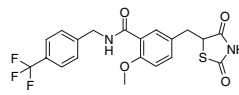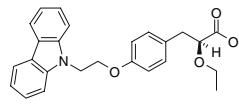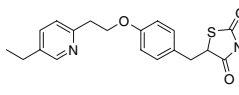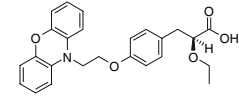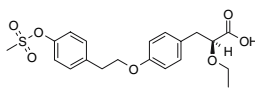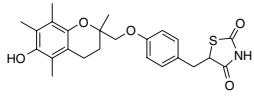
B. Results

1. *PPAR agonists*. 321 ligands that activate PPARs were investigated. For more than one third of all PPAR agonists (36%) the PPAR target was ranked first (Fig. 8).

If the PPAR target did not obtain the highest score, in the vast majority of cases (21% of all PPAR agonists) the target cytochrome P450 2C9 (P450 2C9) received the first rank. Interestingly, P450 2C9 represents an enzyme involved in the metabolism of PPAR ligands [28]. Moreover, the six models for the P450 2C9 target comprised in the Inte:Ligand database are not as restrictive as our PPAR models, because the P450 2C9 hypotheses were made to accommodate a highly diverse set of ligands which are metabolized by this enzyme [29]. Taking into account these facts, the high ranking of the P450 2C9 target using PPAR agonists as queries can be explained. For 30 PPAR activators (9%) the target human rhinovirus (HRV) coat protein was ranked first. Natural ligands of the HRV coat protein ligand binding pocket are fatty acids and lipids [30]. Fatty acids are also ligands for PPARs. Therefore, it could be possible that some PPAR agonists are able to fit into the hydrophobic pockets of both, PPAR and HRV coat protein. On that account, we searched for structural similarities between the corresponding PPAR agonists. First, we found out that all 30 PPAR agonists mapped by HRV coat protein models were agonists for PPAR-α and that none of them belonged to the six fatty acids from the PPAR ligand test set. Second, we noticed that all of them could be assigned to three structurally similar groups: The (2R)-2-methylchromane-2-carboxylic acid derivatives, the 2,3-dihydrobenzofuran-2-carboxylic acid analogues, and the propionic acid derivatives [31–33].

In consideration of these facts, it should be interesting to experimentally test these three PPAR agonist classes for HRV coat protein activity. However, some of these models

Table 6 HipHop compound set used for the generation of the *PPAR-γ agonist model* consisting of 14 PPAR-γ agonists

264908-13-6[#]

$EC_{50} = 0.4\ \mu M$ [36]

651724-09-3[#]

$EC_{50} = 0.01\ \mu M$ [37]

853652-40-1[#]

$EC_{50} = 0.07\ \mu M$ [9]

BRL48482

$EC_{50} = 0.013\ \mu M$ [38]

BVT13

$EC_{50} = 1.3\ \mu M$ [39]

CLX-M1

$EC_{50} = 0.28\ \mu M$ [40]

GW409544

$EC_{50} = 0.00028\ \mu M$ [7]

farglitazar

$EC_{50} = 0.00034\ \mu M$ [41]

KRP297

$EC_{50} = 0.8\ \mu M$ [8]

NNC61-4424

$EC_{50} = 0.17\ \mu M$ [42]

pioglitazone

$EC_{50} = 0.58\ \mu M$ [43]

ragaglitazar

$EC_{50} = 0.6\ \mu M$ [8]

tesaglitazar

$EC_{50} = 1.3\ \mu M$ [8]

troglitazone

$EC_{50} = 0.54\ \mu M$ [44]

[#] CAS number of the compound

Table 7 Database search results for the PPAR-γ agonist model

PPAR-γ agonists (%)[a]	Inactives (%)[b]	Enrichment factor
33	1.06	24

[a] Percentage of PPAR-γ agonists found in the 135 PPAR-γ agonists including subset of the PPAR ligands test set

[b] Percentage of inactive drug-like compounds retrieved from our 12775 compounds containing virtual database
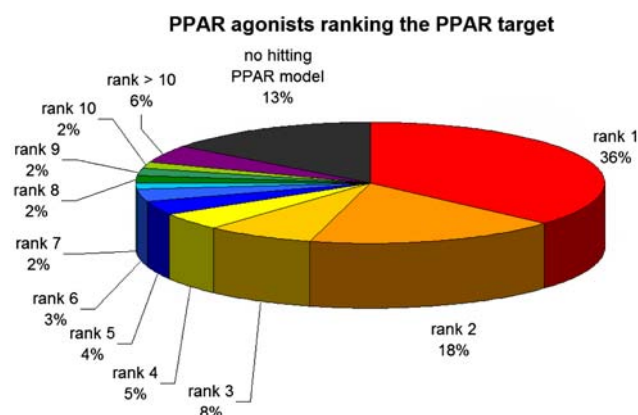

Fig. 8 Frequency of the ranks for the PPAR target. For over 36% of the PPAR agonists the PPAR target was ranked first

were recognized as promiscuous, because they consist of only four hydrophobic features and one or two hydrogen bond acceptors and therefore retrieve a large number of hits in 3D database searches [30].

The target retinoid X receptor beta (RXR-β) got the first rank for 13 PPAR agonists (4%). Our RXR-β models were derived from the PDB entries 1xv9 and 1xvp, both containing pentadecanoic acid as crystal structure ligand and therefore designed to match up fatty acids. Indeed, two of the 13 PPAR agonists were fatty acids. Considering the fact that fatty acids are natural activators of both, PPARs and RXRs, it can be explained that some PPAR agonists were also able to map RXR-β models.

Apart from PPARs and RXR-β, our in-house database included 13 further targets that were members of the nuclear hormone receptor family. Only two of them, pregnane X receptor (PXR) and estrogen receptor alpha (ER-α), were ranked first for one and two ligands, respectively.

Forty-seven (13%) of the agonists did not match up any PPAR hypotheses. The majority of these non-matching ligands belonged to three groups of PPAR agonists: Dithiolane analogues (12 ligands), clofibric acid derivatives (nine ligands), and benzoxazinone analogues (six ligands). All dithiolane analogues were not able to fit to a PPAR hypothesis, whereas three clofibric acid derivatives and 31 benzoxazinone analogues matched up PPAR hypotheses. However, the PPAR target was mostly ranked

low for the matching agonists of the last two groups. This indicates that our PPAR models were too restrictive to accommodate these chemical scaffolds.

2. *PPAR inactives*. 36 compounds from bibliographic data that possess the same scaffolds as known PPAR agonists, but do not bind to PPARs were analyzed. The majority of PPAR inactives (52%) did not fit to any PPAR hypothesis or scored the PPAR target with a rank lower than seven (Fig. 9).

For eleven PPAR inactives (30%) the PPAR target obtained the highest scores, which underscores the high structural similarity of these compounds to PPAR activators (Table 8). The target cytochrome P450 2C9 (P450 2C9) was ranked first for the majority of PPAR inactives (19%) if the PPAR target did not receive the first rank.

Discussion

In the first part of our study, we generated 47 structure-based PPAR models with LigandScout and one ligand-based PPAR hypothesis within Catalyst. To find the best models for PPAR agonists of the three subtypes, a test set including 357 PPAR ligands was screened against all 48 hypotheses.

We show that PPAR-α agonist model 1 is a highly selective tool to find PPAR-α agonists and that the unselective PPAR-α agonist model 2 avoids a lot of false negative hits. PPAR-δ agonist model and PPAR-γ agonist model represent selective templates for activators of the delta and gamma subtype.

In the second part, we determined the target ranking of the 357 PPAR ligands within the Inte:Ligand pharmacophore database to investigate if the pharmacological activity of the ligands was predicted correctly.

Our results show that for more than one third of all PPAR agonists (36%), the PPAR target was ranked first.
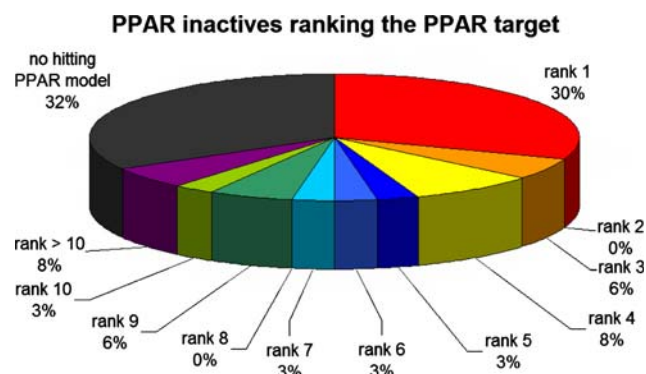

Fig. 9 Ranks for the PPAR target after scoring the 36 PPAR inactives. Nearly, one third of the PPAR inactives was not able to match any PPAR model

P450 2C9, the target with the second highest number of first ranks, takes part in the metabolism of PPAR ligands and was prioritized by about one fifth of all PPAR agonists (21%). Therefore, the PPAR target was more often ranked first than any other target. Other frequently first ranked targets—HRV coat protein (9%) and RXR-β (4%)—represented a target for compounds that possessed a similar binding mode as PPAR ligands.
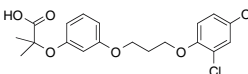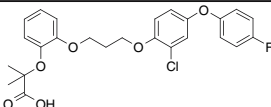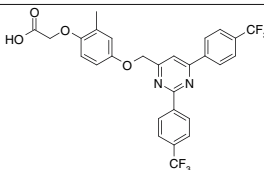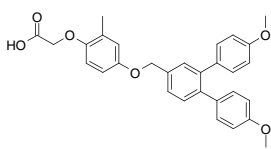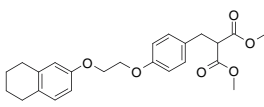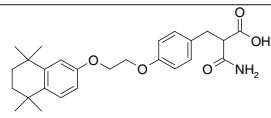
Among the 15 targets of the nuclear hormone receptor family in our in-house database, the PPAR target was ranked first in the majority of cases. Only a small number of PPAR agonists preferred the RXR-β target and for three PPAR agonists ER-α and PXR were ranked first. Thus, except for RXR-β, targets from the PPAR including receptor family did not show a significant enrichment for PPAR agonists.

Nearly one third of the PPAR inactives did not match up any PPAR hypotheses. However, PPAR inactives ranked the PPAR target more often first than other targets. Due to the lack of activity information for these "inactives" on other PPAR subtypes than the one published, we cannot exclude that these ligands are not able to activate other PPAR subtypes. Therefore, some of these putative PPAR inactives for which PPAR was the first ranked target, could actually be activators for other PPAR subtypes that were not mentioned in the bibliographic data. Moreover, biological activity of a compound not only depends on its

ability to bind to the active site of the protein, but also on the permeability of the ligand through cell walls and thus the availability at the target expression site. On that account, it can be difficult to distinguish structural closely related PPAR inactives from their active analogues using pharmacophore models.

According to these results, parallel screening represents a suitable in silico method for finding the biological target for a set of compounds. However, it should be mentioned that parallel screening is not a fully automated process, since the structure-based pharmacophore models used for forecasting the biological activity of ligands are refined manually to improve their selectivity. Therefore, the accuracy of the pharmacological activity prediction for a set of ligands depends on the discriminatory power of the refined models. For example, a model that was refined by deleting all but two features in order to retrieve more training set compounds, would be too promiscuous and would therefore match a multitude of structurally diverse ligands which are not biological active on the pharmacological target that the model represents. On that account, for a multitude of ligands, this target would obtain a high score and therefore an early rank, although it is not the pharmacological correct target. This would lead to false ligand activity predictions in a parallel screen. Thus, only pharmacophore models which were generated and refined using standard operating procedures—such as using a

Table 8 Structures of some PPAR agonists and their corresponding inactive analogues

PPAR agonist	PPAR inactive
882176-04-7[#]	882176-05-8[#]
PPAR-α: EC$_{50}$ = 0.036 μM, ref. [33]	ref. [33]
870289-66-0[#]	890137-45-8[#]
PPAR-δ: EC$_{50}$ = 0.03 μM, ref. [45]	ref. [45]
701979-40-0[#]	701294-94-2[#]
PPAR-γ: EC$_{50}$ = 1.5 μM, ref. [46]	ref. [46]

[#] CAS number of the compound

minimum number of four features including at least one non-hydrophobic feature (ionizable feature, charged feature, or hydrogen bond feature) for one model, default settings for the Catalyst feature definitions and only utilizing shape features derived from the ligand of the PDB ligand–protein complex—can be considered to be included into the pharmacophore database. Moreover, the analysis of the prioritized targets for a set of ligands has to be performed by an expert with knowledge about the quality of the pharmacophore models representing the targets. Otherwise, results for some targets like the HRV coat protein that includes models which contain mostly hydrophobic features and therefore retrieve large hit lists in database searching, would be overestimated.

Conclusion

In summary, our large scale study on pharmacophore modeling and parallel screening for PPAR ligands leaves us with two conclusions: First, our 48 PPAR models represent a highly restrictive set of pharmacophore filters. Second, our recently introduced parallel screening approach gave promising results, because the PPAR agonists were able to prioritize the PPAR target within a 1537 pharmacophore models including database comprising 181 pharmacological targets. This verifies the use of parallel screening for determining the—in terms of biological activity—correct target for a set of compounds.

Supplementary material

Structures of the PPAR agonists of the four training sets and of the 357 PPAR ligand test set compounds.

References

1. Xu HE, Lambert MH, Montana VG, Parks DJ, Blanchard SG, Brown PJ, Sternbach DD, Lehmann JM, Wisely GB, Willson TM, Kliewer SA, Milburn MV (1999) Mol Cell 3:397
2. Blaschke F, Takata Y, Caglayan E, Law RE, Hsueh WA (2006) Arterioscler Thromb Vasc Biol 26:28
3. Cabrero A, Llaverias G, Roglans N, Alegret M, Sanchez R, Adzet T, Laguna JC, Vazquez M (1999) Biochem Biophys Res Commun 260:547
4. Burgermeister E, Schnoebelen A, Flament A, Benz J, Stihle M, Gsell B, Rufer A, Ruf A, Kuhn B, Marki HP, Mizrahi J, Sebokova E, Niesor E, Meyer M (2006) Mol Endocrinol 20:809
5. Willson TM, Brown PJ, Sternbach DD, Henke BR (2000) J Med Chem 43:527
6. Tenenbaum A, Motro M, Fisman EZ (2005) Cardiovasc Diabetol 4:14
7. Xu HE, Lambert MH, Montana VG, Plunket KD, Moore LB, Collins JL, Oplinger JA, Kliewer SA, Gampe RTJ, Mckee DD, Moore JT, Willson TM (2001) Proc Natl Acad Sci USA 98:13919
8. Ebdrup S, Pettersson I, Rasmussen HB, Deussen HJ, Frost JA, Mortensen SB, Fleckner J, Pridal L, Nygaard L, Sauerberg P (2003) J Med Chem 46:1306
9. Mahindroo N, Wang CC, Liao CC, Huang CF, Lu IL, Lien TW, Peng YH, Huang WJ, Lin YT, Hsu MC, Lin CH, Tsai CH, Hsu JT, Chen X, Lyu PC, Chao YS, Wu SY, Hsieh HP (2006) J Med Chem 49:1212
10. Wolber G, Langer T (2005) J Chem Inf Model 45:160
11. Oberfield JL, Collins JL, Holmes CP, Goreham DM, Cooper JP, Cobb JE, Lenhard JM, Hull-Ryde EA, Mohr CP, Blanchard SG, Parks DJ, Moore LB, Lehmann JM, Plunket K, Miller AB, Milburn MV, Kliewer SA, Willson TM (1999) Proc Natl Acad Sci USA 96:6102
12. Kapoor A, Kashaw SK, Saxena AK (2004) Med Chem Res 13:770
13. Rathi L, Kashaw SK, Dixit A, Pandey G, Saxena AK (2004) Bioorg Med Chem 12:63
14. Xu XY, Cheng F, Shen JH, Luo XM, Chen LL, Yue LD, Du Y, Ye F, Jiang SH, Zhu DY, Jiang HL, Chen KX (2003) Int J Quantum Chem 93:405
15. Iwata Y, Miyamoto S, Takamura M, Yanagisawa H, Kasuya A (2001) J Mol Graph Model 19:536–542
16. Steindl TM, Schuster D, Laggner C, Langer T (2006) J Chem Inf Model 46:2146
17. Pipeline Pilot, 5.0.1.100. Scitegic, 10188 Telesis Court., Suite 100, San Diego, CA 92121, USA
18. Catalyst, Version 4.11. Accelrys, 9685 Scranton Road, San Diego, CA 92121, USA
19. Berman HM, Westbrook J, Feng Z, Gilliland G, Bhat TN, Weissig H, Shindyalov IN, Bourne PE (2000) Nucleic Acids Res 28:235
20. Derwent World Drug Index 2003. Scientific, T., 3501 Market Street, Philadelphia, PA 19104, USA
21. ilib:diverse, 1.0.2. Inte:Ligand, Clemens Maria Hofbauer-G. 6, A-2344 Maria Enzersdorf, Austria
22. Schuster D, Laggner C, Steindl TM, Palusczak A, Hartmann RW, Langer T (2006) J Chem Inf Model 46:1301
23. Jacobsson M, Lidén P, Stjernschantz E, Boström H, Norinder U (2003) J Med Chem 46:5781
24. Hecker EA, Duraiswami C, Andrea TA, Diller DJ (2002) J Chem Inf Comput Sci 42:1204
25. Diller DJ, Li R (2003) J Med Chem 46:4638
26. Clement OO, Mehl AT (2000) International University Line: La Jolla 71
27. Steindl T, Langer T (2004) J Chem Inf Comput Sci 44:1849
28. Karanam BV, Hop CE, Liu DQ, Wallace M, Dean D, Satoh H, Komuro M, Awano K, Vincent SH (2004) Drug Metab Dispos 32:1015
29. Schuster D, Laggner C, Steindl TM, Langer T (2006) Curr Drug Discov Technol 3:1
30. Steindl TM, Crump CE, Hayden FG, Langer T (2005) J Med Chem 48:6250
31. Koyama H, Boueres JK, Miller DJ, Berger JP, Macnaul KL, Wang PR, Ippolito MC, Wright SD, Agrawal AK, Moller DE, Sahoo SP (2005) Bioorg Med Chem Lett 15:3347
32. Shi GQ, Dropinski JF, Zhang Y, Santini C, Sahoo SP, Berger JP, Macnaul KL, Zhou G, Agrawal A, Alvaro R, Cai TQ, Hernandez M, Wright SD, Moller DE, Heck JV, Meinke PT (2005) J Med Chem 48:5589
33. Desai RC, Metzger E, Santini C, Meinke PT, Heck JV, Berger JP, Macnaul KL, Cai TQ, Wright SD, Agrawal A, Moller DE, Sahoo SP (2006) Bioorg Med Chem Lett 16:1673

34. Fyffe SA, Alphey MS, Buetow L, Smith TK, Ferguson MA, Sorensen MD, Bjorkling F, Hunter WN (2006) J Mol Biol 356:1005

35. Takada I, Yu RT, Xu HE, Lambert MH, Montana VG, Kliewer SA, Evans RM, Umesono K (2000) Mol Endocrinol 14:733

36. Yanagisawa H, Takamura M, Yamada E, Fujita S, Fujiwara T, Yachi M, Isobe A, Hagisawa Y (2000) Bioorg Med Chem Lett 10:373

37. Rybczynski PJ, Zeck RE, Dudash JJ, Combs DW, Burris TP, Yang M, Osborne MC, Chen X, Demarest KT (2004) J Med Chem 47:196

38. Willson TM, Cobb JE, Cowan DJ, Wiethe RW, Correa ID, Prakash SR, Beck KD, Moore LB, Kliewer SA, Lehmann JM (1996) J Med Chem 39:665

39. Ostberg T, Svensson S, Selen G, Uppenberg J, Thor M, Sundbom M, Sydow-Backman M, Gustavsson AL, Jendeberg L (2004) J Biol Chem 279:41124

40. Arlt W, Neogi P, Gross C, Miller WL (2004) J Mol Endocrinol 32:425

41. Trifilieff A, Bench A, Hanley M, Bayley D, Campbell E, Whittaker P (2003) Br J Pharmacol 139:163

42. Sauerberg P, Pettersson I, Jeppesen L, Bury PS, Mogensen JP, Wassermann K, Brand CL, Sturis J, Woldike HF, Fleckner J, Andersen AS, Mortensen SB, Svensson LA, Rasmussen HB, Lehmann SV, Polivka Z, Sindelar K, Panajotova V, Ynddal L, Wulff EM (2002) J Med Chem 45:789

43. Liu KG, Lambert MH, Ayscue AH, Henke BR, Leesnitzer LM, Oliver WRJ, Plunket KD, Xu HE, Sternbach DD, Willson TM (2001) Bioorg Med Chem Lett 11:3111

44. Henke BR, Blanchard SG, Brackeen MF, Brown KK, Cobb JE, Collins JL, Harrington WWJ, Hashim MA, Hull-Ryde EA, Kaldor I, Kliewer SA, Lake DH, Leesnitzer LM, Lehmann JM, Lenhard JM, Orband-Miller LA, Miller JF, Mook RAJ, Noble SA, Oliver WJ, Parks DJ, Plunket KD, Szewczyk JR, Willson TM (1998) J Med Chem 41:5020

45. Epple R, Azimioara M, Russo R, Bursulaya B, Tian SS, Gerken A, Iskandar M (2006) Bioorg Med Chem Lett 16:2969

46. Li Z, Liao C, Ko BC, Shan S, Tong EH, Yin Z, Pan D, Wong VK, Shi L, Ning ZQ, Hu W, Zhou J, Chung SS, Lu XP (2004) Bioorg Med Chem Lett 14:3507